JVI Journals.ASM.org

Hepatitis C Virus Nonstructural Protein 5B Is Involved in Virus Morphogenesis

Hamed Gouklani,[a,b] Rowena A. Bull,[c] Claudia Beyer,[a] Fasséli Coulibaly,[d] Eric J. Gowans,[a] Heidi E. Drummer,[a,b] Hans J. Netter,[b] Peter A. White,[c] and Gholamreza Haqshenas[a,b]

The Macfarlane Burnet Institute for Medical Research and Public Health, Melbourne, Victoria, Australia[a]; Department of Microbiology, Monash University, Clayton, Victoria, Australia[b]; School of Biotechnology and Biomolecular Sciences, University of New South Wales, Sydney, Australia[c]; and Department of Biochemistry, Monash University, Clayton, Victoria, Australia[d]

The p7 protein of hepatitis C virus (HCV) is a viroporin that is dispensable for viral genome replication but plays a critical role in virus morphogenesis. In this study, we generated a JFH1-based intergenotypic chimeric genome that encoded a heterologous genotype 1b (GT1b) p7. The parental intergenotypic chimeric genome was nonviable in human hepatoma cells, and infectious chimeric virions were produced only when cells transfected with the chimeric genomes were passaged several times. Sequence analysis of the entire polyprotein-coding region of the recovered chimeric virus revealed one predominant amino acid substitution in nonstructural protein 2 (NS2), T23N, and one in NS5B, K151R. Forward genetic analysis demonstrated that each of these mutations *per se* restored the infectivity of the parental chimeric genome, suggesting that interactions between p7, NS2, and NS5B were required for virion assembly/maturation. p7 and NS5B colocalized in cellular compartments, and the NS5B mutation did not affect the colocalization pattern. The NS5B K151R mutation neither increased viral RNA replication in human hepatoma cells nor altered the polymerase activity of NS5B in an *in vitro* assay. In conclusion, this study suggests that HCV NS5B is involved in virus morphogenesis.

Hepatitis C virus (HCV) is classified in the *Hepacivirus* genus of the family *Flaviviridae* and encodes a polyprotein of ~3,000 amino acids that is cleaved into at least 10 mature proteins by cellular and viral proteases (43). The three major structural proteins—core and the E1 and E2 glycoproteins (gp)—form viral particles, and the nonstructural (NS) proteins NS2 to NS5 and p7 are required for viral genome replication and virus morphogenesis (19, 30).

The recent discovery of the ability to cultivate HCV in cell culture (HCVcc) has provided opportunities to investigate and characterize the roles of the HCV structural and NS proteins in virus morphogenesis. The p7 protein is not required for RNA replication (4, 19, 25, 46) but is indispensable for infectious virion formation (15, 19, 46). p7 is a viroporin and forms functional ion channels in artificial lipid bilayers (11, 13, 35, 40). In cultured cells, p7 modulates the acidic pH of the classic secretory pathway and protects acid-labile intracellular HCV particles (50). The presence of an HXXXW motif similar to that found in the prototype viroporin, influenza virus M2, further indicates that p7 may function as a proton channel (29, 38). In addition to its ion channel activity, increasing data suggest that p7 is a multifunctional protein and plays a role in virus assembly through interaction with other viral proteins. Among the viral proteins, core and NS2 have been reported to interact with p7 during infectious virion formation (18, 26, 33, 39). Identification of other viral proteins that interact with p7 during virus morphogenesis will lead to a better understanding of the function of p7 and may identify novel antiviral targets for the treatment of hepatitis C.

The HCV NS2 protein of 217 amino acids is an endoplasmic reticulum (ER) membrane-associated multifunctional protein that has at least one transmembrane (TM) domain (42, 51). During polyprotein processing, NS2 is cleaved from the precursor p7-NS2 protein by a cellular signal peptidase, and this process is modulated by the p7 sequence (7). The C terminus of NS2, independently of its N terminus, functions as a viral protease and, in conjunction with NS3, cleaves the NS2-NS3 junction, resulting in the production of two mature proteins, NS2 and NS3. The cleavage of NS2 from NS3 is essential for RNA replication, presumably due to the requirement of a free N terminus for a functional NS3. NS2 and p7 contain TM domains that anchor them to the ER (15, 51). Several reports suggest functional and physical interactions between p7 and NS2 during virus morphogenesis (18, 26, 39). However, there is no report suggesting a possible association between these two proteins and NS5B in virus morphogenesis.

The NS5B protein is an RNA-dependent RNA polymerase (RdRp) that is responsible for HCV RNA replication. The three-dimensional (3-D) structure of NS5B has been determined by several research groups (3, 5, 23, 44). Like other viral RNA polymerases, NS5B contains a putative nucleoside triphosphate (NTP) tunnel through which the NTPs reach the catalytic domain of the enzyme and are utilized for the synthesis of new viral RNA. Several viral NS proteins have been suggested to play a role in HCV assembly/maturation (32), but as yet there is no report indicating such a role for HCV NS5B.

The initial aim of this study was to generate an intergenotypic chimeric virus that encodes the amantadine-sensitive p7 protein of genotype 1b (GT1b) (strain J4) (11, 12). However, the replication-competent parental chimeric genome was assembly defective and required several passages to produce infectious virus. Nucleotide sequencing of the genomes of recovered viruses revealed

Received 15 December 2011 **Accepted** 9 February 2012
Published ahead of print 15 February 2012
Address correspondence to Gholamreza Haqshenas, haqshenas@yahoo.com.

doi:10.1128/JVI.07089-11

mutations in p7, NS2, and NS5B. Analysis of these mutations suggested an association between these proteins and provided an opportunity to investigate the role of HCV NS5B in virus morphogenesis.

MATERIALS AND METHODS

Cells, plasmids, and antibodies. Dulbecco's modified Eagle's medium (DMEM; Gibco/BRL, Gaithersburg, MD) was used to culture the Huh7-derived HL1 cells and Huh7.5 cells (kindly provided by F. Chisari [Scripps Research Institute, La Jolla, CA]) as described previously (15). Constructs containing the cDNA of the wild-type JFH1 genome (pJFH1) and its replication-defective version (pJFH1-GND) were kindly provided by T. Wakita (49). The anti-E2 monoclonal antibody (MAb) AP33 (34) was kindly provided by A. Patel, University of Glasgow, Glasgow, United Kingdom. Jc1FLAG2(p7-nsGluc2a) (28), referred to as Jc1-Luc in this study, and anti-NS5A MAb 9E10 (34) were kindly provided by C. Rice (The Rockefeller University, New York, NY). Jc1-Luc is a modified version of Jc1 (37) that encodes a luciferase gene at the p7-NS2 junction, and the Flag epitope has been fused to the E2 N terminus. A rabbit anti-myc polyclonal antibody and mouse anti-Flag MAb M2 were purchased from Santa Cruz Biotechnology and Sigma-Aldrich, respectively.

RT-PCR and sequencing analysis. To sequence the entire HCV genome, total RNA was extracted from the culture supernatant fluids as described previously (13, 15). cDNA synthesis and amplification were performed using a one-step reverse transcription-PCR (RT-PCR) kit (Invitrogen) according to the manufacturer's instructions. The BigDye Terminator kit (Applied Biosystems) and virus-specific oligonucleotides were used to sequence PCR products and cloned cDNA fragments directly.

Construction of recombinant plasmids. The construction of the intermediate recombinant plasmid 5′JFH-Fp7 has been described elsewhere (13). This construct contains the 5′ untranslated region (5′ UTR) and the core, E1, E2, and partial NS2 genes from wild-type JFH1 and a full-length or partial p7 gene from an Australian isolate of HCV GT1b (HCV-A) (48). The p7 proteins of HCV-A and J4 differ by two amino acids located in the cytosolic loop and TM domain 2 (TM2), respectively (13). Using overlapping PCR, point mutations were introduced into the 5′JFH-Fp7 plasmid to generate the mutant construct 5′JFH-J4p7, and the sequence was confirmed by automated cycle sequencing. The construct was subsequently digested with EcoRI and KpnI, and the fragment containing the 5′ UTR, core, E1, E2, p7, and partial NS2 genes was substituted for the corresponding fragment of pJFH1. The resultant construct was designated JFH1-J4p7, and the nucleotide sequence of p7 was confirmed as described previously (13).

Recombinant plasmids containing wild-type p7 and NS5B or the NS5B mutant were constructed using standard molecular biology techniques. Overlapping PCR was used to introduce the point mutation into NS5B. PCR was used to amplify the p7 and NS5B genes from pJFH1and pHCV-A (48). The Kozak sequence and the translation initiation codon (ATG) were engineered at the 5′ ends of the coding regions. The translation stop codon (TGA) was inserted at the 3′ ends of the coding sequences. To facilitate the detection of viral proteins, either a myc or a Flag epitope sequence was engineered at their N or C termini via a linker sequence (glycine-serine-glycine-serine [GSGS]). The resultant constructs were named pJFH1p7-Flag (JFH1 p7 fused to the Flag epitope sequence at its 3′ end), Hp7-Flag (HCV-A p7 fused to the Flag epitope sequence at its 3′ end), myc-NS5B (JFH1 NS5B fused to the myc epitope sequence at its 5′ end), and myc-NS5BKR (myc-NS5B encoding the K151R mutation). The oligonucleotides used for the generation of these constructs are available upon request. The fragments were cloned into a pcDNA3.1 plasmid (Invitrogen) under the control of the cytomegalovirus (CMV) promoter sequence. To measure the polymerase activity of JFH1 NS5B using an *in vitro* assay, the NS5B region was PCR amplified and cloned into pTrcHis2C (Invitrogen, Mount Waverley, Australia) as described previously (21). The K151R mutation was introduced into the wild-type NS5B gene using conventional site-directed mutagenesis.

Mutagenesis of NS2 and NS5B in pJFH1. Overlapping PCR was used to introduce single and double mutations into the wild-type and chimeric JFH1 cDNA sequences. The sequences of the oligonucleotides used in these experiments are available upon request. The final mutated constructs were designated T23N-W (W identifies wild-type JFH1) and T23N-J (J identifies JFH1-J4p7). By a similar strategy, the K151R mutation was introduced into the SnaBI-BsrGI fragments of pJFH1 and JFH1-J4p7 NS5B. The mutated fragments were cleaved with SnaBI and BsrGI and were substituted for the SnaBI-BsrGI fragments of pJFH1 and JFH1-J4p7. The final constructs were named K151R-W and K151R-J, respectively. To generate wild-type and JFH1-J4p7 constructs encoding both T23N and K151R, the EcoRI-KpnI fragment of K151R-J was replaced by the corresponding fragment from T23N-W or T23N-J, and the resultant mutant was designated T23N/K151R-W or T23N/K151R-J, respectively.

***In vitro* RNA transcription and transfection.** RNA transcripts from HCV cDNA were generated as described previously (13, 15). Briefly, linearized HCV cDNA was used to synthesize *in vitro* transcripts using either a MEGAscript kit (Ambion) or an AmpliScribe T7 high-yield transcription kit (Epicentre Biotechnologies, Madison, WI). Using DMRIE-C transfection reagent (Invitrogen), 6 μg RNA was transfected into HL1 cells as described previously (13, 15).

IF and immunoblot analyses. Immunofluorescence (IF) and immunoblot analyses were performed as described previously (13, 15). An anti-NS5A MAb and anti-E2 MAb AP33 were used to detect transfected and infected cells. To visualize the bound antibodies, an Alexa Fluor 488-conjugated goat anti-mouse antibody (Molecular Probes) was used. Propidium iodide or Hoechst stain was used to counterstain cell nuclei, and the cells were examined with a Bio-Rad or Nikon laser confocal microscope.

Immunoblot analysis was carried out as described previously (15). Briefly, 4×10^5 HL1 cells were cultured overnight and were transfected with 4 μg wild-type or chimeric transcripts. At 48 h posttransfection, cells were washed with cold phosphate-buffered saline (PBS) and were lysed by adding 50 μl 2× Laemmli buffer (Bio-Rad, Hercules, CA). The lysates were homogenized by passage through a 25-gauge needle and were denatured at 100°C for 5 min. The proteins were subsequently resolved on a 10% sodium dodecyl sulfate-polyacrylamide gel electrophoresis (SDS-PAGE) gel and were transferred to a polyvinylidene difluoride (PVDF) membrane. The membranes were sequentially exposed to the following antibodies: goat polyclonal anti-core (ViroStat, Portland, ME), mouse anti-E2 MAb AP33, and a mouse anti-NS5A MAb, at dilutions of 1/500, 1/2,000, and 1/10,000, respectively. The bound primary antibodies were detected using appropriate horseradish peroxidase (HRP)-conjugated secondary antibodies and ECL Western blotting detection reagents (Amersham Pharmacia Biosciences) according to the manufacturers' instructions.

Virus preparation and titration. At the indicated time points posttransfection, the supernatant fluids were collected and filtered through 0.45-μm-pore-size filters. To determine the viral titers by using IF, HL1 cells were grown overnight on coverslips and were infected with diluted samples. At 48 h postinfection, the cells were stained with an anti-E2 or anti-NS5A MAb, and the bound antibodies were detected as described above. The number of foci of IF-positive cells was counted when it was between 10 and 100 per coverslip, and the viral infectivity titer was expressed as focus-forming units (FFU) per milliliter. To determine the effects of the identified mutations on virus infectivity, cells grown in duplicated wells were transfected with each RNA, and the supernatant fluids were inoculated into duplicate wells. The average number of focus-forming units (FFU) for the four wells was calculated. To determine intracellular infectivity, viral particles bound to the cell membranes were removed by trypsinization, and the cells were lysed by four freeze-thaw cycles. The lysates were clarified by low-speed centrifugation and filtration, as described above.

Colocalization experiments. Colocalization experiments were performed as described previously (15). Briefly, to investigate the colocalization of p7 and NS5B and the effects of NS5B K151R on the colocalization pattern, the constructs encoding the p7-Flag and myc-NS5B proteins (1 μg each) were cotransfected into 8×10^4 Huh7.5 cells that had been cultured overnight. At 48 h posttransfection, cells were fixed and permeabilized with paraformaldehyde and Triton X-100, respectively. The expressed tagged proteins were detected using a mouse anti-myc MAb (Invitrogen) and a rabbit anti–Flag polyclonal antibody at 1/1,000 dilutions. Alexa Fluor 594-conjugated goat anti-mouse IgG and Alexa Fluor 488-conjugated goat anti-rabbit IgG were used to detect p7 and NS5B using laser confocal microscopy.

Quantification of HCV core protein. To measure extra- and intracellular core quantities, we used the Ortho HCV antigen enzyme-linked immunosorbent assay (ELISA) kit (Ortho Clinical Diagnostics, Inc., Tokyo, Japan). HL1 cells were transfected with viral transcripts as described above, and the culture supernatant fluids and cells were collected at 72 h posttransfection. Culture supernatant fluids and cell lysates were diluted 1/10 and 1/1,000, respectively, before they were used in the assay. The amounts of core were calculated according to the manufacturer's instructions. The average quantities of duplicate samples were calculated and were normalized to the core quantities of wild-type JFH1.

RNA replication analysis. The quantifiable luciferase encoded by the HCV genome has been used as a surrogate to quantify RNA replication (28, 46). To generate HCV RNA encoding luciferase, the *Renilla* luciferase gene encoding the first four amino acids of NS2 (YDAP) at its N terminus was cloned at the p7-NS2 junction as described for the J6/JFH1 chimera (19). The foot-and-mouth disease virus (FMDV) autoproteolytic peptide 2A was engineered at the C terminus of luciferase to ensure the cleavage of luciferase from NS2. Jc1-Luc was used as a positive control for luciferase activity. A total of 7×10^4 HL1 or Huh7.5 cells were seeded into 48-well tissue culture plates, and the overnight-cultured cells were transfected with 0.5 μg (per well) wild-type and chimeric JFH1 transcripts encoding the luciferase gene (in triplicate for each transcript). At 24, 48, and 72 h posttransfection, intracellular luciferase activity was measured using the *Renilla* luciferase assay system (Promega) and a FLUOstar microplate reader (BMG LabTechnologies). To lyse the cells, 70 μl of *Renilla* lysis buffer was added to each well, and 20 μl of this buffer was used in the assay as described in the manufacturer's instructions.

***In vitro* polymerase activity assay.** Plasmids containing mutated or wild-type NS5B were transformed into *Escherichia coli* BL21 cells by heat shock for expression as described previously (21). HCV JFH1 NS5B was purified as described previously (6). In brief, cells were collected by centrifugation and were lysed by sonication. The soluble fraction was loaded onto a Hi-Trap column (Amersham Biosciences, Buckinghamshire, United Kingdom) charged with Ni^{2+}, and the histidine-tagged recombinant polymerase was eluted using a binding buffer containing increasing concentrations of imidazole from 50 to 500 mM. The recombinant polymerase was buffer exchanged and was stored at −80°C. The polymerase activities of the wild-type and mutant NS5B proteins were measured as described previously (6). Briefly, assays were performed in a final volume of 15 μl that contained 20 mM Tris-HCl (pH 7.4), 2.5 mM $MnCl_2$, 5 mM dithiothreitol (DTT), 1 mM EDTA, 500 ng of homopolymeric C RNA template, 2 U RNasin (Promega), 4 mM sodium glutamate, and increasing concentrations of [^{3}H]GTP (Amersham Biosciences, Little Chalfont, United Kingdom) ranging from 2 μM to 60 μM. Reactions were initiated by the addition of 100 nM NS5B, and reaction mixtures were incubated for 20 min at 25°C. The radiolabeled RNA was precipitated on ice for 30 min and was filtered through a 96-well GF/C unifilter microplate (Falcon, Franklin Lakes, NJ), and radioactivity was measured by scintillation spectrometry. Results were plotted and analyzed in GraphPad Prism, version 5.0c (GraphPad Software, San Diego, CA).

Computer modeling. The crystal structure of JFH1 NS5B deposited in the Protein Data Bank (PDB) (identifier 3i5k) (44) was used to represent the effects of point mutations visualized with PyMOL software (www.pymol.org). The ConSurf server (10) was used to map sequence conservation on the 3-D structure of NS5B structural subdomains.

RESULTS

The replication-competent parental chimeric JFH1 genome encoding the mutated HCV-A p7 was assembly defective, and infectious virus was secreted with a delay. A JFH1-based p7 intergenotypic chimeric cDNA construct encoding HCV-A p7 containing two mutations was constructed (Fig. 1A). Consistent with our published data (13), the parental chimeric genome was noninfectious, and infectious virions were recovered only after two passages of transfected cells, allowing mutation of the chimeric transcripts (Fig. 1B). Additionally, we demonstrated that Huh7 and HL1 cells transfected with the replication-competent JFH1 mutants either lacking the p7 gene or encoding two mutations in the p7 cytosolic loop (R33I and R35S) failed to secrete infectious virus into supernatant fluids for six consecutive passages (data not shown). To investigate whether the production or secretion of infectious chimeric viral particles in the transfected cells was impaired, intracellular infectivity was assessed. The latter experiment demonstrated that the chimeric genomes did not produce intracellular infectious virions (see Fig. 4). Because HCV particles are infectious in the early steps of virus production and do not require further maturation during virus release for their infectivity (9), our data suggest that the replacement of JFH1 p7 by the HCV-A p7 mutant impaired early steps of infectious virus production. The data presented above do not show whether the cells transfected with the chimeric genomes produced noninfectious viral particles. To determine whether the same numbers of viral particles were produced and released from transfected cells regardless of their infectivity, we assessed the core protein quantities in the cells and culture supernatant fluids at 72 h posttransfection. As can be seen from Fig. 1C, HL1 cells transfected with the intergenotypic chimeric genome secreted less than 20% of the amount of core protein secreted by the wild type. Intracellular core quantities of cells transfected with the chimeric genome were 60% greater than those of cells transfected with the wild type, demonstrating that the reduction in the secreted core quantity was not due to lower production of this protein by the chimeric genome. Because HCV-A p7, like JFH1 p7, has ion channel activity (13), the results presented above, taken together, suggested that the defect in infectious virus production by the chimeric genome was due to incompatibility between p7 and the other viral proteins.

The replication of the intergenotypic chimeric genome is comparable to that of the wild type, and the corresponding polyprotein is processed efficiently. The defect in infectious virus production could be due to insufficient replication of the intergenotypic chimeric genome. The RNA remaining after transfection did not allow us to measure RNA replication directly by using standard quantitative RT-PCR techniques. Instead, we used the activity levels of the *Renilla* luciferase inserted at the p7-NS2 junction as a surrogate measure of RNA replication (Fig. 2A) (see Materials and Methods) (19). Following transfection of HL1 cells with equal quantities of the chimeric and wild-type transcripts, the intracellular luciferase activity levels were comparable at different points posttransfection (Fig. 2B). In this experiment, the control Jc1-Luc transcript, encoding a luciferase gene at the p7-NS2 junction, replicated at levels comparable to those of wild-type and chimeric transcripts, but the luciferase activity of GND-Luc,

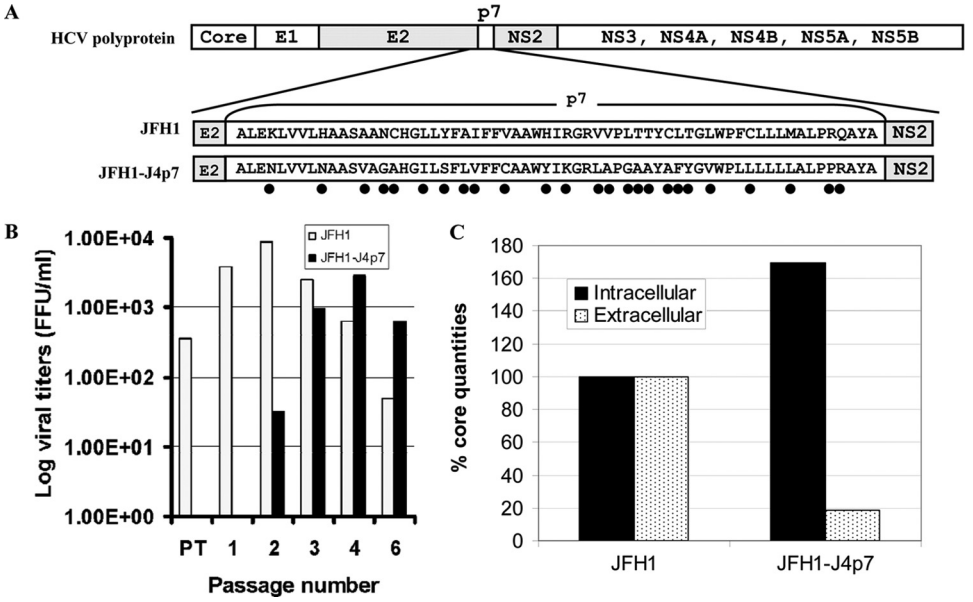

FIG 1 A JFH1-based intergenotypic chimeric genome encoding the mutant p7 protein of HCV-A with an amino acid sequence identical to that of J4 p7 is replication competent but exhibits delayed secretion of infectious virions. (A) Schematic representation of the intergenotypic chimeric JFH1 genome encoding mutant p7 (JFH1-J4p7). The mismatched residues are identified by filled circles. (B). HL1 cells were transfected with wild-type JFH1 and JFH1-J4p7 transcripts. The viral titers in the supernatant fluids collected at 72 h posttransfection (PT) and at passages 1, 2, 3, 4, and 6 were determined (see Materials and Methods). Wild-type JFH1 and JFH1-J4p7 infectivity titers are represented by shaded and filled bars, respectively. FFU, focus-forming units. (C) At 72 h after transfection with JFH1 or JFH1-J4p7, intra- and extracellular core protein quantities were measured and were normalized to JFH1 core quantities as described in Materials and Methods.

encoding a lethal mutation in NS5B, decreased over time. The experiment described above established that wild-type and intergenotypic transcripts replicated at comparable levels and that the failure of infectious virus production by the intergenotypic chimeric transcript was not due to impairment of RNA replication.

The HCV polyprotein is processed into several individual mature proteins posttranslationally. The amino acid sequences flanking p7 appear to affect the cleavage of the E2-p7-NS2 precursor protein (7). Therefore, we investigated whether the replacement of JFH1 p7 by HCV-A p7 adversely affected the processing of the

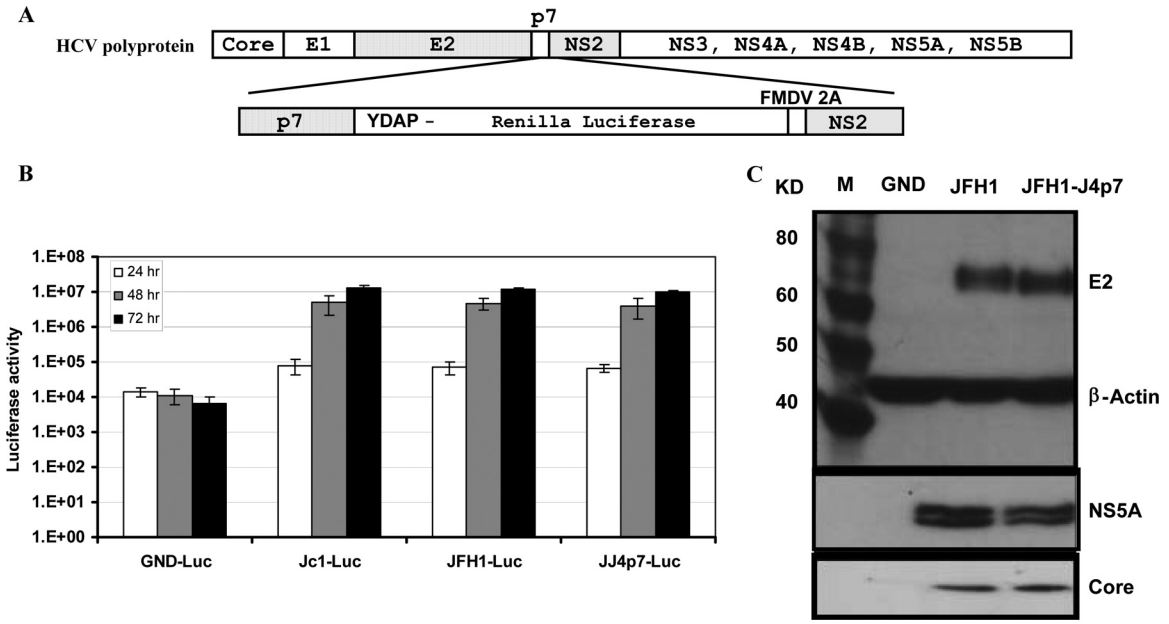

FIG 2 The intergenotypic chimeric genome was fully replication competent, and the encoded polyprotein was processed efficiently. (A) Schematic diagram showing the locations of the luciferase gene and FMDV 2A in the chimeric polyproteins. (B) At 24, 48, and 72 h after the transfection of HL1 cells with GND-Luc, Jc1-Luc, JFH1-Luc, or JFH1-J4p7-Luc transcripts, intracellular luciferase activity was measured as described in Materials and Methods. (C) HL1 cells were transfected with the GND, wild-type JFH1, or JFH1-J4p7 genome. At 48 h posttransfection, the cells were lysed in 2× Laemmli sample buffer, and the viral proteins were resolved onto a 10% SDS-PAGE gel and were detected as described in Materials and Methods. Magic Marker (Invitrogen) was used as size markers.

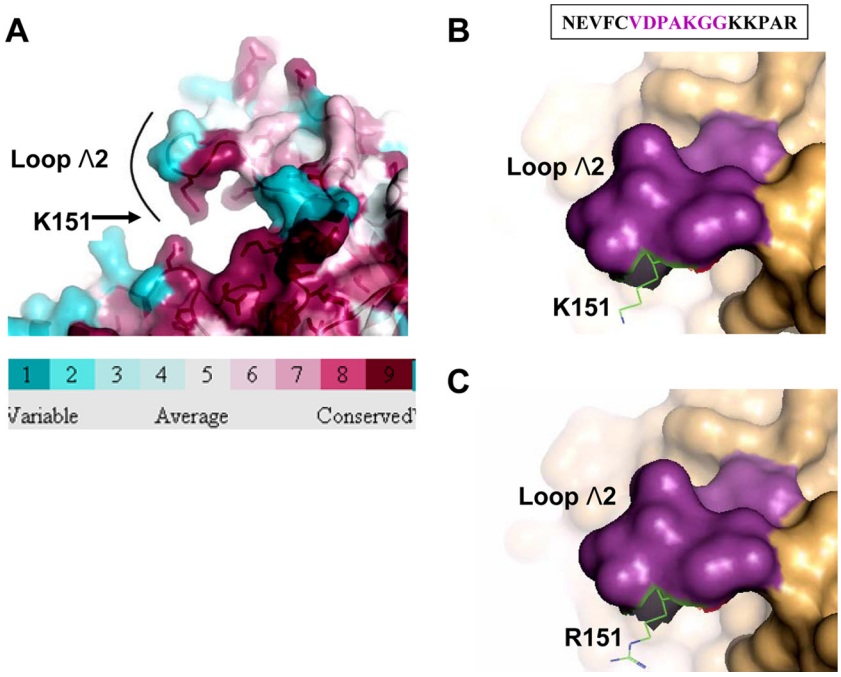

FIG 3 Three-dimensional (3-D) structure of wild-type and mutant JFH1 NS5B proteins. (A) Close view of loop Λ on the NS5B surface. The sequence conservation on the molecular surface is represented by a blue-white-red gradient. ConSurf conservation scores 1 to 9, representing highly variable to highly conserved residues, and the respective colors are shown below the model (ConSurf server). (B and C) The positions of K151 in the wild type (B) and of R151 in the mutant (C) have been shown in the 3-D model of JFH1 NS5B (PDB identifier, 3i5k) (44). The amino acid sequence of loop Λ2 (shown in purple) and a few surrounding amino acids are given above figure B.

precursor protein, which, in turn, may have impaired infectivity. Immunoblot analysis using the anti-E2 MAb AP33 revealed no detectable difference in the processing of the wild-type and chimeric polyproteins (Fig. 2C). In addition, we also detected core and NS5A, which are located at opposite ends of the polyprotein, and further confirmed that the chimeric polyprotein was processed efficiently (Fig. 2C). These data suggest that the impairment of infectious virus production following transfection of the chimeric genomes into HL1 cells was not due to grossly incomplete processing of the chimeric polyprotein. However, we acknowledge the limitation in the sensitivity of immunoblot analysis and therefore cannot rule out the possibility of minor differences in the processing of the wild-type and chimeric polyproteins.

Rescued mutant viruses harbor compensatory mutations in NS2 and NS5B. The defect in virus production by the chimeric JFH1 genomes suggests that the compatibility of p7 and other viral proteins is crucial for virus assembly/maturation. In addition, the emergence of the revertant viruses after passaging of the cells harboring the chimeric genomes indicated the possible emergence of a compensatory mutation(s) in the defective genomes that suppressed the assembly defect and restored their infectivity. To identify point mutations in the genomes of chimeric viruses, viral stocks were prepared by infecting HL1 cells with supernatants from passages 4 and 2 of wild-type JFH1 and JFH1-J4p7, respectively. The infected cells were passaged once, and their supernatant fluids were filtered and were used as the viral stocks. To determine the nucleotide sequences of JFH1 and the chimeras, the entire coding regions of the wild-type and chimeric genomes were amplified by RT-PCR in seven overlapping fragments and were sequenced. Alignment of the nucleotide sequences of the recovered virus with the parental genome revealed mutations at two positions, 2847 and 8118, that resulted in two amino acid changes in two viral proteins, NS2 and NS5B, respectively. The mutation at position 2847 (C2847A) resulted in the replacement of a threonine residue at position 836 in the polyprotein (position 23 in JFH1 NS2) by an asparagine in the putative NS2 TM1. Residue 23 of NS2 is highly conserved among GT2, GT5, and GT6 (http://euhcvdb.ibcp.fr/euHCVdb/), with a conservative mutation to serine in GT1, GT3, and GT4. In addition to the mutation in NS2, a nonsynonymous mutation at position 8118 (A8118G) was observed, resulting in the replacement of lysine at position 2593 in the polyprotein (position 151 in JFH1 NS5B) by an arginine residue. Both arginine and lysine have positively charged side chains, but the guanidium group of arginine is planar and can participate in a variety of stacking interactions. Residue K151 in NS5B is highly conserved among all HCV genotypes. It is one of the residues lining the NTP tunnel and, along with six adjacent amino acids (positions 147 to 153), forms loop Λ2 at the inlet of the NTP tunnel (5, 44) (Fig. 3). Modeling suggests that the K151R mutation does not result in significant alterations in the overall structure of the protein.

Point mutations in NS2 and NS5B restored the infectivity of defective chimeric genomes. The sequencing results suggested that point mutations in NS2 and NS5B could have corrected the incompatibility between these proteins and the mutant HCV-A p7. Recently, we have demonstrated that the C2847A mutation in NS2 was sufficient for the restoration of the infectivity of a chimeric genome encoding wild-type HCV-A p7 (H. Gouklani et al., submitted for publication). To investigate the effects of the identified mutations on the restoration of the infectivity of the chimeric genomes, RNAs from JFH1, parental JFH1-J4p7, T23N-J (J

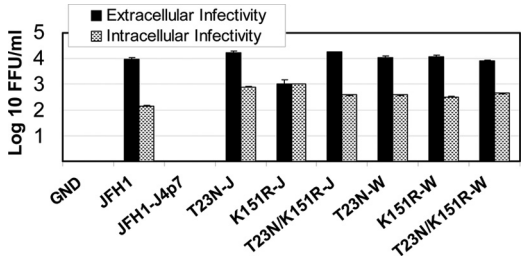

FIG 4 Compensatory mutations in NS2 and NS5B promoted virus production from assembly-defective chimeric genomes. Site-directed mutagenesis was used to introduce point mutations encoding T23N and K151R into NS2 and NS5B, respectively. HL1 cells were transfected with replication-incompetent GND, wild-type genomes (JFH1), chimeric genomes (JFH1-J4p7), chimeric genomes encoding NS2 T23N (T23N-J), chimeric genomes encoding NS5B K151R (K151R-J), chimeric genomes encoding NS2 T23N and NS5B K151R (T23N//K151R-J), wild-type genomes encoding NS2 T23N (T23N-W), wild-type genomes encoding NS5B K151R (K151R-W), or wild-type genomes encoding NS2 T23N and NS5B K151R (T23N//K151R-W). At 48 h posttransfection, the supernatant fluids were collected, and their infectivity was determined and expressed as focus-forming units (FFU) per milliliter of supernatant as described in Materials and Methods.

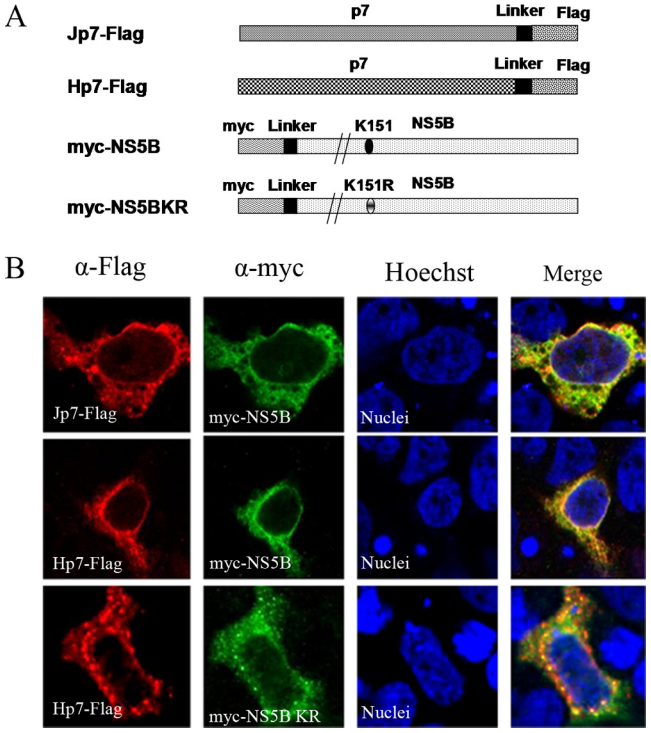

FIG 5 Colocalization of p7 and NS5B. (A) Schematic representations of the constructs that were utilized to express JFH1 p7 tagged with the Flag epitope (Jp7-Flag), HCV-A p7 tagged with the Flag epitope (Hp7-Flag), JFH1 NS5B tagged with the myc epitope (myc-NS5B), and JFH1 NS5B containing K151R tagged with the myc epitope (myc-NS5BKR). (B) At 48 h after transfection of Huh7.5 cells with the constructs diagramed in Fig. 5A, cells were fixed with paraformaldehyde, and the tagged proteins were detected using antibodies to the Flag (α-Flag) and myc (α-myc) epitopes as described in Materials and Methods. Laser confocal microscopy was used to visualize the proteins in the cells. (Top) Colocalization of JFH1 p7-Flag and myc-NS5B. (Center) Colocalization of HCV-A p7 and myc-NS5B. (Bottom) Colocalization of HCV-A p7 and myc-NS5BKR. The nuclei were stained with Hoechst stain.

refers to JFH1-J4p7), T23N-W (W refers to wild-type JFH1), K151R-W, K151R-J, T23N/K151R-W, and T23N/K151R-J were transfected into HL1 cells. At 48 h postinfection, the culture supernatant fluids of the transfected cells were used to infect naïve HL1 cells. Anti-NS5A IF revealed that both mutations *per se* restored the infectivity of the nonviable genomes (Fig. 4). None of the mutations enhanced infectivity over that of the wild-type virus. To investigate the functional roles of the mutations, we measured intracellular infectivity and showed a direct correlation between intracellular and extracellular infectivity for the wild type and the NS2 mutant (Fig. 4). Interestingly, the mutant containing the NS5B mutation revealed intracellular infectivity similar to that of the wild type but extracellular infectivity 10-fold lower than that of the wild type. This suggests that the NS5B mutation alone did not efficiently correct the defect in virus assembly and secretion. An alternative explanation would be that intracellular infectivity did not reach a threshold level allowing virus secretion.

The p7 protein colocalizes with NS5B in subcellular compartments. Recent publications indicate that p7 and NS2 interact physically and that this interaction is critical for virus production (18, 26, 39). Cross-genotype interactions of p7 and NS2 have also been reported (39). We have also demonstrated recently that HCV-A p7 and JFH1 NS2 colocalize in cellular compartments (Gouklani et al., submitted). Following the determination of genetic interactions between p7 and NS5B (see above), we investigated whether these two proteins colocalized in cells as a prerequisite for their genetic and functional interactions. For this purpose, p7-Flag and myc-NS5B were transiently expressed in Huh7.5 cells. JFH1 p7-Flag and JFH1 myc-NS5B colocalized in an ER-like pattern that was particularly evident in the perinuclear region (Fig. 5). We also demonstrated that HCV-A p7-Flag and JFH1 myc-NS5B colocalized in the same pattern as that observed for JFH1 p7 and NS5B. Although we did not observe any alteration in the colocalization of NS5B and p7, we further tested whether JFH1 NS5B K151R had an impact on the colocalization of p7 and NS5B. The latter experiment demonstrated that the K151R mutation in NS5B did not affect the colocalization pattern of p7 and NS5B, although the NS5B mutant, compared to the wild type, appeared as distinct dots (Fig. 5).

Single point mutations did not alter RNA replication. The rescue of nonviable chimeric genomes by single point mutations in NS2 and NS5B could be due to the enhancement of viral RNA replication. Therefore, we investigated whether the introduction of point mutations had an impact on RNA replication. For this purpose, the *Renilla* luciferase activity was measured as a surrogate marker for viral RNA replication, as described in Materials and Methods. Following transfection of the same quantities of the respective transcripts into HL1 cells (in triplicate for each transcript), intracellular luciferase activity was measured at 24, 48, and 72 h posttransfection. As can been seen from Fig. 6, the mutants encoding the NS2 T23N and NS5B K151R mutations replicated efficiently, and we did not observe a remarkable difference between the replication of parental chimeric genomes and that of genomes carrying mutations in NS2 and NS5B. The Jc1-Luc transcript, which was used as a positive control, also produced levels of luciferase activity comparable to those of the wild type and the chimeric transcripts encoding point mutations (Fig. 6). However, when the cells were transfected with GND-Luc, which is replication defective, significantly lower levels of luciferase activity were observed. This experiment suggested that the individual point

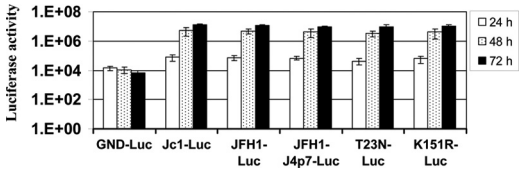

FIG 6 The point mutations identified did not alter RNA replication. The point mutations were introduced into the wild type (JFH1-Luc) and JFH1-J4p7-Luc as described for Fig. 2. HL1 cells were transfected with equal quantities of transcripts, and intracellular luciferase activity was measured at 24, 48, and 72 h posttransfection. Jc1-Luc and GND-Luc acted as positive and negative controls, respectively. T23N-Luc, JFH1-J4p7-Luc encoding the T23N mutation; K151R-Luc, JFH1-J4p7-Luc encoding the K151R mutation.

mutations had no effect on viral RNA replication and that the rescue of the nonviable intergenotypic transcript was not due to an increase in RNA replication.

NS5B K151R did not alter NS5B polymerase activity, suggesting a role for NS5B in virus morphogenesis. Several HCV NS proteins have been reported to play a role in virus assembly (32). In this study, we demonstrated that the NS5B K151R mutation rescued the assembly-defective virus, while it did not alter viral genome replication. To further investigate the effects of K151R on NS5B polymerase activity, an *in vitro* system was used as described previously (6). As can be seen in Table 1, the wild-type NS5B and the mutant revealed the same catalytic efficiency (k_{cat}/K_m), suggesting that, consistent with the cell culture system results, K151R did not alter NS5B polymerase activity.

DISCUSSION

In this study, we generated a JFH1 chimeric genome that encoded a heterologous p7 with an amino acid sequence identical to that of the p7 protein of the J4 strain. J4 p7 has been shown to form amantadine-sensitive ion channels *in vitro* (11, 12, 47). We identified two point mutations in NS2 and NS5B that corrected a detrimental incompatibility between these proteins and p7. Further characterization of the NS5B mutation suggested a role for NS5B in virus assembly.

Until recently, due to the lack of an *in vitro* propagation system, HCV assembly and maturation steps had been poorly characterized. The introduction of HCVcc provided a unique opportunity for the elucidation of the mechanisms of virus assembly (24, 49, 53). For the first time, using HCVcc, it has been demonstrated that NS proteins NS2, NS3, NS4B, NS5A, and p7 are involved in HCV assembly and maturation (2, 15–17, 19, 20, 27, 30, 46). The involvement of NS proteins in virus assembly is one of the unique characteristics of the family *Flaviviridae* (32). Viroporin p7 is essential for virus replication *in vivo* and *in vitro* (19, 41, 46). Several studies suggest that p7 is a multifunctional protein and, independently of its ion channel activity, plays a role in virus assembly. It has been reported that a GT1-based intergenotypic chimeric genome encoding a functional GT2 p7 was nonviable in chimpanzee (41). In addition, in our current and previous studies, we demonstrated that replacement of JFH1 p7 with heterologous p7 genes with functional ion channel activity failed to produce intra- or extracellular infectious virions (13). These experiments suggested that p7 contained structural determinants that interact with other viral proteins during virus assembly. The identification of point mutations in NS2 and NS5B revealed an association between these proteins and p7 during virus morphogenesis. The failure to detect intracellular infectivity, along with the reduction of core protein release from cells transfected with chimeric genomes, indicated that the association of p7, NS2, and NS5B is required for a crucial step in infectious virus production and release. Recently, using the newly developed HCVcc, several research groups reported that full-length NS2 and its two putative N-terminal TM domains play an essential role in HCV morphogenesis and maturation (19, 36, 52). NS2 interacts with several viral proteins, including E1-E2 gp, p7, NS3, and NS5A, during virus assembly (18, 26, 39, 45). Our recent results (Gouklani et al., submitted) and the present study confirm critical interactions between p7 and NS2. In the present study, it was also demonstrated that the NS5B K151R mutation corrected an assembly defect in virus morphogenesis through functional interactions with a heterologous p7. Lysine 151 is highly conserved among all HCV strains. Interestingly, a lysine exists at the corresponding position in the NS5B protein of GB virus B (GBV-B) (GenBank accession number NC_001655), which is a close genetic relative of HCV and infects New World monkeys, tamarins and marmosets (14, 31). K151 is located on the molecular surface of NS5B in the finger domain of the protein, and it constitutes the first positively charged amino acid of the NTP tunnel (22). However, a mass spectrometric protein footprinting approach demonstrated that K151 did not interact with the viral RNA during RNA replication (8). In addition, mutagenesis analysis of K151 revealed that replacement of this residue by a neutral amino acid (alanine) had only a subtle effect on RNA synthesis, suggesting that K151 is dispensable for the delivery of NTPs to the active site of the protein (22). Consistent with the data presented above, we demonstrated that the replacement of K151 with arginine, another positively charged amino acid, had no effect on RNA replication and RdRp activity, suggesting that K151 plays a regulatory role in the virus life cycle. HCV NS5B is indispensable for viral RNA synthesis. As yet, there is no report indicating a role for HCV RdRp in virus assembly. However, it has been reported that the RdRp of bovine viral diarrhea virus (BVDV), a virus of the *Pestivirus* genus in the family *Flaviviridae* that is closely related to HCV, is involved in virus assembly (1). Here, for the first time, we report a role for HCV NS5B in virus assembly through interaction with p7. Because the K151R mutation did not abolish wild-type virus production, despite the high conservation of K151 among all HCV GTs, we believe that the entire Λ2 loop might be involved in virus assembly. Further studies are required to demonstrate the exact function of K151 in the HCV life cycle.

Recently, we have demonstrated that p7, core, NS2, and NS5A contribute to a distinct step in virus morphogenesis (Gouklani et al. submitted). The current study indicates that this step in assembly/maturation may also involve NS5B. In conclusion, these results suggest that a multiprotein complex links the RNA synthe-

TABLE 1 Catalytic efficiencies of wild-type and mutant NS5B proteins

	NS5B K151R		Wild-type NS5B	
Measurement (unit)	Mean	SD	Mean	SD
V_{max} (mol/μg/h)	1.45E−11	6.80E−12	2.97E−11	2.73E−11
k_{cat} (s^{-1})	3.50E−04	1.64E−04	7.17E−04	6.60E−04
K_m (M)	8.57E−06	9.05E−06	1.84E−05	2.08E−05
k_{cat}/K_m (M^{-1} s^{-1})	4.09E+01	1.81E+01	3.91E+01	3.18E+01

sis machinery to virus assembly and that p7 may play a key role in this process.

ACKNOWLEDGMENTS

We thank T. Wakita for the JFH1 and GND-JFH1 cDNA plasmids. We also thank Charles Rice (The Rockefeller University, New York, NY) for the monoclonal antibody to NS5A and for Jc1FLAG2(p7-nsGluc2a). We thank Arvind Patel (University of Glasgow) for kindly providing the anti-E2 monoclonal antibody AP33. We also thank C. Jones (The Rockefeller University, New York, NY) for help in the construction of the JFH1 reporter virus. We appreciate Paul Ramsland of the Burnet Institute for critical discussions.

This study was supported by grants from the National Health and Medical Research Council (NH&MRC), an NH&MRC Career Development Award, the Australian Centre for HIV & Hepatitis (ACH2), and the CASS Foundation.

REFERENCES

1. **Ansari IH, et al.** 2004. Involvement of a bovine viral diarrhea virus NS5B locus in virion assembly. J. Virol. **78**:9612–9623.
2. **Appel N, et al.** 2008. Essential role of domain III of nonstructural protein 5A for hepatitis C virus infectious particle assembly. PLoS Pathog. **4**:e1000035.
3. **Biswal BK, et al.** 2005. Crystal structures of the RNA-dependent RNA polymerase genotype 2a of hepatitis C virus reveal two conformations and suggest mechanisms of inhibition by non-nucleoside inhibitors. J. Biol. Chem. **280**:18202–18210.
4. **Blight KJ, Kolykhalov AA, Rice CM.** 2000. Efficient initiation of HCV RNA replication in cell culture. Science **290**:1972–1974.
5. **Bressanelli S, et al.** 1999. Crystal structure of the RNA-dependent RNA polymerase of hepatitis C virus. Proc. Natl. Acad. Sci. U. S. A. **96**:13034–13039.
6. **Bull RA, Eden JS, Rawlinson WD, White PA.** 2010. Rapid evolution of pandemic noroviruses of the GII.4 lineage. PLoS Pathog. **6**:e1000831.
7. **Carrere-Kremer S, et al.** 2004. Regulation of hepatitis C virus polyprotein processing by signal peptidase involves structural determinants at the p7 sequence junctions. J. Biol. Chem. **279**:41384–41392.
8. **Deval J, et al.** 2007. High resolution footprinting of the hepatitis C virus polymerase NS5B in complex with RNA. J. Biol. Chem. **282**:16907–16916.
9. **Gastaminza P, et al.** 2008. Cellular determinants of hepatitis C virus assembly, maturation, degradation and secretion. J. Virol. **82**:2120–2129.
10. **Glaser F, et al.** 2003. ConSurf: identification of functional regions in proteins by surface-mapping of phylogenetic information. Bioinformatics **19**:163–164.
11. **Griffin SD, et al.** 2003. The p7 protein of hepatitis C virus forms an ion channel that is blocked by the antiviral drug, Amantadine. FEBS Lett. **535**:34–38.
12. **Griffin SD, et al.** 2004. A conserved basic loop in hepatitis C virus p7 protein is required for amantadine-sensitive ion channel activity in mammalian cells but is dispensable for localization to mitochondria. J. Gen. Virol. **85**:451–461.
13. **Haqshenas G, Dong X, Ewart G, Bowden S, Gowans EJ.** 2007. A 2a/1b full-length p7 inter-genotypic chimeric genome of hepatitis C virus is infectious in vitro. Virology **360**:17–26.
14. **Haqshenas G, Dong X, Netter HJ, Toressi J, Gowans EJ.** 2007. A chimeric GB virus B encoding the hepatitis C virus hypervariable region 1 is infectious in vivo. J. Gen. Virol. **88**:895–902.
15. **Haqshenas G, Mackenzie JM, Dong X, Gowans EJ.** 2007. Hepatitis C virus p7 protein is localized in the endoplasmic reticulum when it is encoded by a replication-competent genome. J. Gen. Virol. **88**:134–142.
16. **Hughes M, Griffin S, Harris M.** 2009. Domain III of NS5A contributes to both RNA replication and assembly of hepatitis C virus particles. J. Gen. Virol. **90**:1329–1334.
17. **Jirasko V, et al.** 2008. Structural and functional characterization of nonstructural protein 2 for its role in hepatitis C virus assembly. J. Biol. Chem. **283**:28546–28562.
18. **Jirasko V, et al.** 2010. Structural and functional studies of nonstructural protein 2 of the hepatitis C virus reveal its key role as organizer of virion assembly. PLoS Pathog. **6**:e1001233.
19. **Jones CT, Murray CL, Eastman DK, Tassello J, Rice CM.** 2007. Hepatitis C virus p7 and NS2 proteins are essential for production of infectious virus. J. Virol. **81**:8374–8383.
20. **Jones DM, Patel AH, Targett-Adams P, McLauchlan J.** 2009. The hepatitis C virus NS4B protein can *trans*-complement viral RNA replication and modulates production of infectious virus. J. Virol. **83**:2163–2177.
21. **Jones LA, Clancy LE, Rawlinson WD, White PA.** 2006. High-affinity aptamers to subtype 3a hepatitis C virus polymerase display genotypic specificity. Antimicrob. Agents Chemother. **50**:3019–3027.
22. **Labonte P, et al.** 2002. Modulation of hepatitis C virus RNA-dependent RNA polymerase activity by structure-based site-directed mutagenesis. J. Biol. Chem. **277**:38838–38846.
23. **Lesburg CA, et al.** 1999. Crystal structure of the RNA-dependent RNA polymerase from hepatitis C virus reveals a fully encircled active site. Nat. Struct. Biol. **6**:937–943.
24. **Lindenbach BD, et al.** 2005. Complete replication of hepatitis C virus in cell culture. Science **309**:623–626.
25. **Lohmann V, et al.** 1999. Replication of subgenomic hepatitis C virus RNAs in a hepatoma cell line. Science **285**:110–113.
26. **Ma Y, et al.** 2011. Hepatitis C virus NS2 protein serves as a scaffold for virus assembly by interacting with both structural and nonstructural proteins. J. Virol. **85**:86–97.
27. **Ma Y, Yates J, Liang Y, Lemon SM, Yi M.** 2008. NS3 helicase domains involved in infectious intracellular hepatitis C virus particle assembly. J. Virol. **82**:7624–7639.
28. **Marukian S, et al.** 2008. Cell culture-produced hepatitis C virus does not infect peripheral blood mononuclear cells. Hepatology **48**:1843–1850.
29. **Meshkat Z, Audsley M, Beyer C, Gowans EJ, Haqshenas G.** 2009. Reverse genetic analysis of a putative, influenza virus M2 HXXXW-like motif in the p7 protein of hepatitis C virus. J. Viral Hepat. **16**:187–194.
30. **Miyanari Y, et al.** 2007. The lipid droplet is an important organelle for hepatitis C virus production. Nat. Cell Biol. **9**:1089–1097.
31. **Muerhoff AS, et al.** 1995. Genomic organization of GB viruses A and B: two new members of the *Flaviviridae* associated with GB agent hepatitis. J. Virol. **69**:5621–5630.
32. **Murray CL, Jones CT, Rice CM.** 2008. Architects of assembly: roles of *Flaviviridae* non-structural proteins in virion morphogenesis. Nat. Rev. Microbiol. **6**:699–708.
33. **Murray CL, Jones CT, Tassello J, Rice CM.** 2007. Alanine scanning of the hepatitis C virus core protein reveals numerous residues essential for production of infectious virus. J. Virol. **81**:10220–10231.
34. **Owsianka A, et al.** 2005. Monoclonal antibody AP33 defines a broadly neutralizing epitope on the hepatitis C virus E2 envelope glycoprotein. J. Virol. **79**:11095–11104.
35. **Pavlovic D, et al.** 2003. The hepatitis C virus p7 protein forms an ion channel that is inhibited by long-alkyl-chain iminosugar derivatives. Proc. Natl. Acad. Sci. U. S. A. **100**:6104–6108.
36. **Phan T, Beran RK, Peters C, Lorenz IC, Lindenbach BD.** 2009. Hepatitis C virus NS2 protein contributes to virus particle assembly via opposing epistatic interactions with the E1–E2 glycoprotein and NS3–NS4A enzyme complexes. J. Virol. **83**:8379–8395.
37. **Pietschmann T, et al.** 2006. Construction and characterization of infectious intragenotypic and intergenotypic hepatitis C virus chimeras. Proc. Natl. Acad. Sci. U. S. A. **103**:7408–7413.
38. **Pinto LH, Lamb RA.** 2006. Influenza virus proton channels. Photochem. Photobiol. Sci. **5**:629–632.
39. **Popescu CI, et al.** 2011. NS2 protein of hepatitis C virus interacts with structural and non-structural proteins towards virus assembly. PLoS Pathog. **7**:e1001278.
40. **Premkumar A, Wilson L, Ewart GD, Gage PW.** 2004. Cation-selective ion channels formed by p7 of hepatitis C virus are blocked by hexamethylene amiloride. FEBS Lett. **557**:99–103.
41. **Sakai A, et al.** 2003. The p7 polypeptide of hepatitis C virus is critical for infectivity and contains functionally important genotype-specific sequences. Proc. Natl. Acad. Sci. U. S. A. **100**:11646–11651.
42. **Santolini E, Pacini L, Fipaldini C, Migliaccio G, Monica N.** 1995. The NS2 protein of hepatitis C virus is a transmembrane polypeptide. J. Virol. **69**:7461–7471.
43. **Shimotohno K, et al.** 1995. Processing of the hepatitis C virus precursor protein. J. Hepatol. **22**:87–92.
44. **Simister P, et al.** 2009. Structural and functional analysis of hepatitis C virus strain JFH1 polymerase. J. Virol. **83**:11926–11939. 19740982
45. **Stapleford KA, Lindenbach BD.** 2011. Hepatitis C virus NS2 coordinates

virus particle assembly through physical interactions with the E1-E2 glycoprotein and NS3-NS4A enzyme complexes. J. Virol. **85**:1706–1717.
46. **Steinmann E, et al.** 2007. Hepatitis C virus p7 protein is crucial for assembly and release of infectious virions. PLoS Pathog. **3**:e103.
47. **StGelais C, et al.** 2007. Inhibition of hepatitis C virus p7 membrane channels in a liposome-based assay system. Antiviral Res. **76**:48–58.
48. **Trowbridge R, Gowans EJ.** 1998. Molecular cloning of an Australian isolate of hepatitis C virus. Arch. Virol. **143**:501–511.
49. **Wakita T, et al.** 2005. Production of infectious hepatitis C virus in tissue culture from a cloned viral genome. Nat. Med. **11**:791–796.
50. **Wozniak AL, et al.** 2010. Intracellular proton conductance of the hepatitis C virus p7 protein and its contribution to infectious virus production. PLoS Pathog. **6**:e1001087.
51. **Yamaga AK, Ou JH.** 2002. Membrane topology of the hepatitis C virus NS2 protein. J. Biol. Chem. **277**:33228–33234.
52. **Yi M, Ma Y, Yates J, Lemon SM.** 2009. Trans-complementation of an NS2 defect in a late step in hepatitis C virus (HCV) particle assembly and maturation. PLoS Pathog. **5**:e1000403.
53. **Zhong J, et al.** 2005. Robust hepatitis C virus infection in vitro. Proc. Natl. Acad. Sci. U. S. A. **102**:9294–9299.